000138

BOL	FIRST Bolometer	Doc No: BOL/RAL/N0015.01
	Title: **Analysis of FOV response function.**	Date: 17-9-97
	Prepared by: Martin Caldwell	

CIRCULATION:

Martin Caldwell	RAL
Peter Gray	RAL
Tony Richards	RAL
Bruce Swinyard	RAL
Roger Emery	RAL
Matt Griffin	QMW
Eli Atad	ROE

CONTENTS.

Introduction.

To date, the analysis has been limited to propagation of beams through PHOT-BOL and the telescope assuming no clipping occurs subsequent to the telescope. This allows the mirror size required to contain essentially 'all' of the beam (e.g. up to the -30dB truncation point) to be found.

In practice however, it may be impossible to transmit this 'all' of the beam, and in any case, the consequences of successive beam clipping by each component at some higher level, e.g. 1%, may not significantly degrade the FOV response.

This note presents the analysis of clipped beams & the effect on FOV response. The first case considered is clipping at the primary mirror cut-out as this is the most severe case in the current design.

The effect of this clipping on point-source-transmittance (PST) is calculated, while extension to the full FOV is to be made in a later update.

1. Methods for clipped-beam analysis.

Figure 1 shows the important geometry and features to be described.

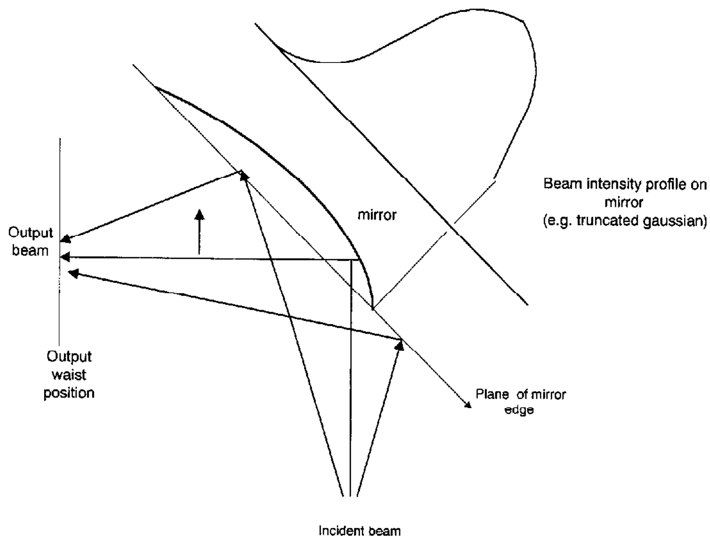

The features needed in the model are:

- Multiple apertures, i.e. beam potentially to be redefined at each component.
- Arbitrary aperture shape.
- Aperture tilt. i.e. beam is clipped in plane shown, which is not perpendicular to beam axis.
- Geometric aberrations.

Previous methods.

The methods known to us are:

1. Fourier analysis.
2. Beam mode analysis.
3. Ray tracing : Field decomposition.

The table below compares the methods in terms of their capabilities..

Capability / Method	Multiple apertures	Aperture shape	Aperture tilt	Geometric aberrations
Fourier analysis (ref.1)	No	Yes	No	No
Beam modes	Yes	Yes (ref.2) but no e.g.'s of non-circular cases	No	Yes, but seldom required (ref.3)
field decomposition	Yes	Yes	Yes	Yes

For this problem the field decompose method is the only one to include all features. For approximate analysis we might use the other methods if they are simpler. For example the beam-mode method can be implemented in ASAP.

1.1 Near/far - field considerations.

1. Although the wavelength is relatively long, most components remain in the far-field region of the beam. E.g. at λ=0.3μm, and typical f-number F= 6, we have gaussian beam waist of $w=2F\lambda/\pi$ =1.14mm, and a beam confocal distance of zo=2Fw = 6.8 mm. As most components are at distances much greater than this from image planes, they are in the far-field. Nevertheless the ray-trace method used is not restricted to far-field portions of the beam. Intermediate and near-field cases are included, except where the beam is focussed. Here the restriction that the analysis pixel size must be greater than 1 wavelength (section 2), means that a different type of ray analysis has to be used.
2. Components at or near image planes are not expected to clip the beam. Because at these positions the beam is more localised, it is always possible to oversize the component adequately. I.e. we assume that as the beam is moved off-axis, it is blocked only by the system field stop (i.e. that which defines the FOV). For stray-light reasons in most cases this is at the detector plane, with all previous field stops being oversized. This assumption can be checked during the ray-trace at each off-axis angle.

Under the above conditions the problem reduces to one of clipping at the non-image plane, not-necessarily pupil-plane, components.

2. Numerical constraints.

It is found that in order to prevent aliasing of the wavefront in the field analysis, it is necessary that the wavefront tilt amounts to less than $\lambda/2$ of path length variation over each pixel. If we take Y as the beam semi-width, and the wave radius of curvature R=2YF, then this requirement implies a minimum analysable wavelength given by $\lambda \geq \frac{Y}{N_{max}.F}$

where N is the maximum number of pixels available.

The maximum analysable wavelength is determined by the requirement that pixel size is greater than the wavelength, i.e. 2Y/N> λ. To increase the allowed range, N may be reduced to some minimum value which is still adequate to describe the beam shape. Therefore the allowed range of wavelenghs is

$$\frac{Y}{N_{max}.F} < \lambda < \frac{2.Y}{N_{min}}$$

For e.g. the BOL photometer with Y≈50mm and max. & min. N values of 255 and 85, we find 0.03mm < λ << 1.2 mm. This just covers the required wavelength range, so we can make the beam analysis. For the actual analysis with tilted components the above equations are modified.

2.1 Resolution of diffracting edges.

The main limitation of the current analysis is that the spatial resolution of the analysis is limited by the requirement that pixel size > λ, i.e. all diffracting edges are 'soft' to a degree equal to one wavelength. For the longest wavelength as used here, this means the edges are almost 2/3mm wide.

3. Detector response models.

It is now asked that the response is modelled for detectors both with and without a 'directivity' in their response, i.e. a sensitivity which varies with direction of the incident flux.

An example of a detector without directivity is that of a bare bolometer which is equally sensitive to light from any direction. The PST in this case is determined by the optical system F-number. In reverse ray-tracing the detector angular response may then be modelled as that of a perfect spherical wave having a 'top-hat' shape in the far field (and therefore an Airy-pattern shape at the detector plane), with size determined by the system F-number. For max. throughput the detector is sized to approximately match the Airy-disc diameter.

A detector with directivity is a bolometer placed behind a Winston cone (ref.6). Here the cone has a cut-off angle θ beyond which light is not transmitted. This requires that the front and rear cone apertures d1 and d2 are related by the equation

$$d2=d1.\sin\theta$$

The front aperture is placed at the image plane and as for the bare detector it is sized to match the Airy disc size of the system F-number. In this case however the F-number is a property of the detector alone, being set by the value of θ. To determine the PST the detector angular response is again modelled as a spherical wave in the far-field, but in this case with an apodization which is not a top-hat shape but which is more rounded or gaussian-like. The cut-off angle θ is actually the 50% intensity point on the far-field beam.

The detector response is so far modelled as a pure gaussian, and the beam propagation and PST calculation is then identical to that for a coherent detector. However, the detector still behaves incoherently, and so to determine the FOV function the PST must still be convolved with the horn geometric footprint, as determined by d1. This is the major distinction between incoherent and coherent detectors, in the case of the latter, the geometric footprint of the detector is not significant.

Since the Winston cone is an incoherent device, its angular response is independent of wavelength. This is valid up to wavelengths such that

$$\lambda/d2 < 1.8$$

(ref.6). Beyond this wavelength the cone is unusable as the rear aperture ceases to transmit energy and the detector efficiency drops.

To model the Winston cone we assume a gaussian angular response. If the angle θ where matched to the system F-number, then the system would clip the beam near the 50% points, which is unacceptable. Instead we assume a cone design such that the main-lobe beam shape at the image plane is approximately equal to that of the Airy pattern case. This is done by making the $1/e^2$ intensity beam waist radius w equal to $2F\lambda/\pi$. The far-field $1/e^2$ divergence angle θdiv is given by

$$\theta div = \lambda/(\pi w)$$
$$=1/(2F)$$

i.e. it is equal to the value of θ for the bare detector case. The acceptance angle of the cone as defined by the 50% beam intensity angle, should be set at

$$\theta = \theta div.\sqrt{(\ln(2)/2)}$$

For BOL with minimum F=5, at the longest wavelength of 0.64mm we have d1≈5mm. The above design implies d2≈0.29mm, giving a cone which could be used only at up to 0.53mm wavelength.

Therefore the above design does not fit the required wavelength range (operation out to 0.64mm) , and will require some adjustment. In particular the actual cone response is not a pure gaussian as assumed here. Also, the relative intensity at the edge of pupil stop of the system is exp(-2)= 13.5 % . This beam sizing is advantageous for minimising clipping, but it may be too much of an 'underfill' with respect to aperture fill factor and hence throughput.

4. FOV models.

4.1. Exact or 'full' model for clipped case.

Strictly the ray-trace should proceed in the forward direction, from source to detector, with the incident beam traced at each off-axis angle (OAA) β, to give the point-source-transmittance (PST(β′), ref.1) where the β′ denotes angular position variable across the detector plane. The FOV response at this angle β is then found from the overlap of PST(β′) with the detector response function (by either incoherent or coherent mixing). This process must be repeated over the OAA range of interest.

In the incoherent detector case, if the dectector size is significant with respect to the Airy disc size, the overlap is accounted for by the convolution of PST(β) with the detector geometric footprint, i.e.

$$FOV(\beta) = \int PST(\beta',\beta) D(\beta').d\beta'$$

where D(β′) is the normalised detector response function.

The ray-trace is usually made in reverse, i.e. the detector response outwards through the system, to give the field u(x) at the entrance aperture. The fourier transform of this field then gives PST(β′,β).

In a case with significant beam clipping the PSF(β′) changes shape with the beam angle β ; for example vignetting causes a reduction in beam size, increasing the Airy disc size. We then have to calculate the PSF as a function of both β and β′, and this is why the ray-trace must be repeated over all β values of interest.

4.2 Simplified model for non-clipped case.

For the case with no clipping, the ray-trace PSF usually has negligible variation with beam angle β, over the range of interest, and in this circumstance only one beam direction β needs to be traced, and the convolution equation becomes

$$FOV(\beta) = \int PST(\beta'-\beta) D(\beta').d\beta'$$

This note gives results for an initial computation of the PSF(β′,β) at the main β angle of interest (that at edge of FOV), for the cases with & without clipping. This gives an initial assessment of the clipping effect.

In the next stage of the work this computation will be repeated over the range of β-values of interest, to map out the actual FOV(β) function over the range of interest.

5. Results.

The beam at one extreme of the PHOT-BOL FOV is propagated, as described in ref.4, from the detector to the sky. In the current design it is expected that all mirrors can be oversized to an edge-taper of -30dB in relative intensity, and so no significant clipping is anticipated in PHOT-BOL itself.

In the telescope however, there are restrictions on the oversize available, the first point at which clipping occurs in the telescope is at the M1 cut-out. Fig.2 shows the beam pattern at this position, including the degree of clipping which arises if the cutout has no oversize, i.e. it is sized to pass only the geometric beam (that defined by the geometric ray-trace). The current model is for a BOL design with FOV placed at the centre of the telescope image plane. Since the degree of clipping is defined not by an absolute size of the component, but by as size relative to the geometric beam, the degree of clipping should be similar in the case of an off-axis BOL when this design is made. The reason we assume no oversize may be possible for this cut-out is that it would drive up the telescope obscuration ratio (there is a need that the secondary mirror is oversized with respect to the cut-out to prevent the straight-thru beam being transmitted). It is unlikely the telescope throughput could be compromised just so as to improve the FOV resolution in the edge detectors in the longest wavelength in just one instrument.

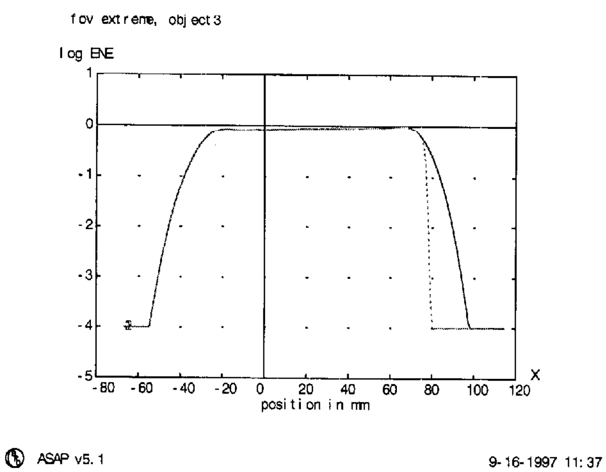

Fig.2 Beam pattern at M1 cut-out. Solid line=unclipped, dotted line=clipped.
Case analysed: Top-hat beam at 0.64mm wavelength.

The effect on the PSF response is found by propagating both the unclipped & clipped beams onto the sky. The resulting response is plotted vs. angle of incidence in fig.3.

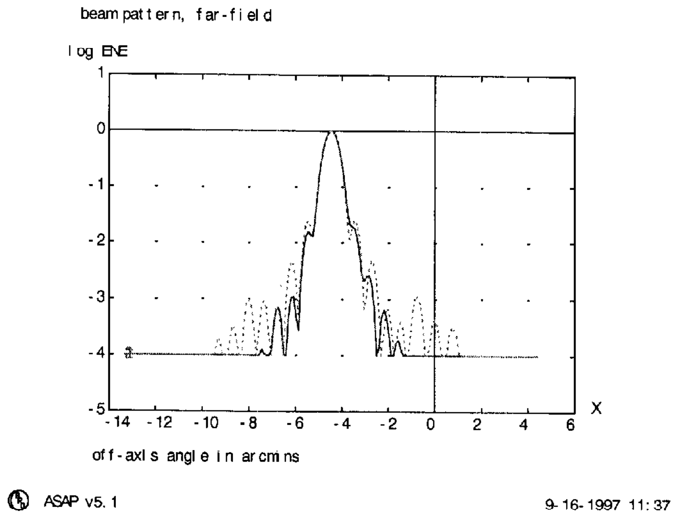

Fig.3. Point source transmittance function PST(β') (beam pattern on sky) showing effect of clipping as per fig.2. (solid line= unclip, dotted=clip).

The effect of the clipping on PSF is small at this β in that it degrades the response mainly in the region outside of the Airy disc, in the 'wings' where it increases the level of at least the first few airy rings. Since these are already at less than the few percent level, the effect of the change may be unimportant, depending on what is the scientific requirement for off-axis rejection ratio. This in turn depends on the ratio of expected signal level and the detector noise level, i.e. the required dynamic range.

A potentially bigger problem is not the FOV response degradation in terms of detector sensitivity on the sky but the detector sensitivity to on-board radiances, for example when the beam pattern is clipped, as well as looking at the portion which continues on out of the instrument, we must investigate the portion which stays behind in the instrument, since much of the instrument is much brighter (hotter) than the sky.

One feature fig.2 reveals is that 2.4 % of the beam pattern views the back of M1 (at 80K). Using the results of ref.5 this would contribute to a direct-emission background ≈ 100% of budget if ε=1. Therefore this surface should if possible not be black.

The accuracy of the above results is limited by the number of rays used in the analysis, which is constrained as described in section 2. The distortion of the Airy ring pattern by the system aberrations is evident in fig.3, and in addition the computation loses accuracy at β-β′ values beyond approx. the first 5 airy rings (in this e.g. it also falls below a threshold of -40dB near this OAA).

References.

Ref.1 "Application of a generalised diffraction analysis to the design of non-standard Lyot-stops for earth-limb viewing radiometers" To be published in Optical Engineering, Oct.'97 issue.
Ref.2 "Mode conversion at diffracting apertures in mm & sub-mm wave optical systems"
Ref.3 "Quasi-optical antennas for radiometric remote-sensing" R J Martin & D H Martin. IEE. Electronics & Communication Engineering Journal. (Feb. 1996).
Ref.4 "Beam patterns in PHOT-BOL design" M Caldwell RAL/BOL/N0006.2.
Ref.5 "Photometer background signal from the optics" A Richards RAL/BOL/N0007.1
Ref.6 "Heat trap: an idealised far-infrared field optics system" D. Harper et al. Appl.Opt. Vol.15,No.1,p.53 (1976).